

Refractive index in the cornea of a harbor porpoise (*Phocoena phocoena*) measured by two-wavelengths laser-interferometry

Ronald H. H. Kröger and Kuno Kirschfeld

Max-Planck-Institut für biologische Kybernetik, Spemannstrasse 38, 72076 Tübingen, Germany

Abstract

The refractive index of the cornea of a harbor porpoise eye was measured by two-wavelengths laser-interferometry. In the thickest part of the cornea a refractive index of about 1.53 was found. From this value, the refractive index gradually decreases to about 1.37 at the surfaces of the cornea. Due to its peculiar shape, the cornea contributes significant, negative refractive power to the overall optics of the eye. The combination of a diverging corneal lens with the powerful, converging crystalline lens results in near emmetropia for the harbor porpoise eye in underwater viewing conditions.

Introduction

It has usually been assumed that in underwater viewing conditions the cornea of cetaceans is scarcely more than a transparent barrier of the eye to the exterior environment. This view was supported by the apparently low refractive index of the cornea (1.3834) measured by Matthiessen (1893) with an Abbe refractometer in the fin whale (*Balaenoptera physalus*). We found about the same values (1.3653 to 1.3960) in the corneas of harbor porpoises (*Phocoena phocoena*) and bottlenose dolphins (*Tursiops truncatus*) (Kröger, 1989) by pressing whole corneas flat on the prism of an Abbe refractometer. A refractive index between 1.365 and 1.385 would render the cornea virtually powerless in water since the adjacent media (water and aqueous humor) have similar refractive indices (ca. 1.339 and 1.336, respectively).

By entirely neglecting the refractive power of the cornea after calculating an extremely long focal length (Matthiessen, 1886) or by using refractive indices of the cornea of about 1.37 (Kröger, 1989), both authors found that in underwater viewing

conditions the harbor porpoise eye should be 5 to 15 diopters myopic (nearsighted) due to the high refractive power of the crystalline lens. Matthiessen (1886) attributed the discrepancy between his calculations and the apparent usefulness of the eyes to the animals to an error in his measurements of the refractive indices within the crystalline lens. However, Matthiessen's indices were successfully used to model the optical properties of the harbor porpoise lens (Kröger, 1989) and are thus likely to be correct.

In most terrestrial mammals, the cornea is relatively thin and varies little in thickness from the axial region to the periphery (e.g. Walls, 1942, Duke-Elder, 1958). In comparison, the harbor porpoise cornea shows extensive thickening in the periphery (Fig. 1). Maximum thickness of the peripheral part of the cornea is about 2 mm while the axial region is about 0.6 to 0.8 mm thick. In water, the thin axial portion of the retina contributes little to the total refraction of rays of light by the optics of the eye since the surfaces of the cornea are almost parallel. In contrast, the angle between the anterior and posterior surface is much larger in the periphery (Fig. 1). Additionally, rays of light travel a longer distance through the cornea. Depending on the refractive index, those thickened areas of the cornea could have a significant effect on the optics of the eye.

Harbor porpoises and other cetacean species have two areas of high ganglion cell density in their retinas roughly aligned on the horizontal meridian of the eye (Dral, 1975, 1977, 1983; Mass *et al.*, 1986; Mass & Supin, 1990). Those areas of maximum retinal resolution translate into two axes of high acuity vision in each eye tilting away from the optical axis in angles of about 50 to 60 degrees. Due to the oblique axes of gaze, the periphery of the cornea is of particular importance. We therefore asked the question whether the refractive index is higher in the periphery of the cornea such that the cornea could act as a diverging lens, as its shape suggests (Fig. 1), and correct the optics of the eye to emmetropia (normalsightedness).

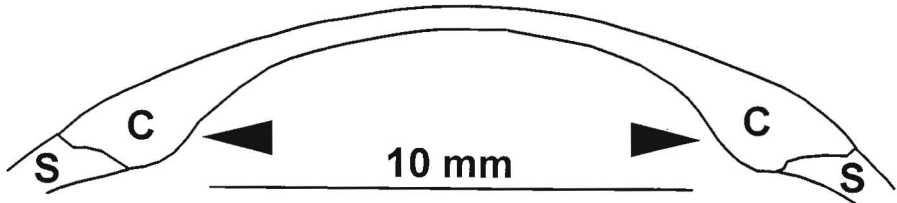


Figure 1. The shape of the harbor porpoise cornea drawn from a naso-temporal cross section. Note the thicker regions in the periphery (arrows). Measurements of refractive index were done in the regions where the C's appear. S=sclera, C=cornea.

A standard interference microscope could not be used to determine refractive indices in cross sections of the cornea since the area of measurement is too small in those instruments. On the other hand, a cornea cross section is a very small sample for an Abbe refractometer. We therefore developed a method that allows determination of refractive indices in samples of intermediate size.

In the thickened, peripheral part of the cornea we found a maximum refractive index of about 1.53. If this high refractive index of the cornea is incorporated into the schematic eyes for the harbor porpoise by Matthiessen (1886) and Kröger (1989), both models predict a refractive state that is close to emmetropia for paraxial optics. If a more detailed analysis of corneal shape and the high index in the interior of the cornea is used in the ray-tracing model of the harbor porpoise eye of Kröger (1989), it predicts a near emmetropic state of refraction over most of the visual field. That is in agreement with observations on the refractive state of the eyes of other small cetaceans in water (Dral, 1972, Dawson *et al.*, 1987a, b). To our knowledge, this is the first account of a vertebrate cornea acting as a diverging lens of physiologically significant refractive power.

Material and methods

The two-wavelengths laser-interferometer

The interferometer was assembled on an optical bench (Spindler & Hoyer). Two laser beams of different wavelengths (543 and 632.8 nm) were combined to a coincident beam with a beamsplitter. The combined beam was purified, widened and splitted into reference and measurement beams. Only the measurement beam passed through the sample while the reference beam remained unchanged. The wavefronts of the reference and measurement beams arrived at the screen slightly tilted to each other, resulting in a regular pattern of interference stripes of adjustable widths. The measurement chamber consisted of two glass plates separated by about 0.2 mm. The maximum area of measurement was about 4 by 12 mm. Interference patterns were

photographed from behind the semi-transparent screen with Kodak Ektachrome 800/1600 film (Fig. 2).

Preparation of cornea samples

Harbor porpoise eyes were obtained from stranded or incidentally netted animals. They were transported and stored in deep-frozen state tightly wrapped into aluminum foil. While an eye was allowed to thaw slowly, the cornea and a small adjacent ring of the sclera were removed. The cornea-sclera preparation was cooled to near 0°C in 0.9% saline solution. Suspended in Tissue-Tek (Miles) that also had been cooled to about 0°C, the cornea was frozen rapidly and cooled to about -20°C.

Naso-temporal cross sections of the cornea were prepared on a cryostat (2800 Frigocut E, Reichert-Jung). Four thickness settings (15, 21, 30, and 42 µm) were used. However, when measured independently, the actual feed of the cryostat was slightly less than indicated: 14.80, 20.13, 29.27, and 39.20 µm, respectively. Care was taken to ensure constant thickness of the slices at a given setting of the cryostat.

One slice at a time was placed into the open measurement chamber and incubated in a moist chamber for about 1 min to remove microscopic gas bubbles trapped in the tissue from freezing. The slice was then covered with a layer of Tissue-Tek, the measurement chamber was closed and inserted into the measurement beam of the interferometer.

The necessary skills in preparing, handling, and measuring corneal sections were developed with a number of harbor porpoise eyes. Harbor porpoises have become rare in European waters and are strictly protected by law in most countries. We therefore had to rely on material from stranded or incidentally netted animals that in most cases is in a poor state of preservation. The results presented here were obtained from an eye that was particularly fresh as judged by visual inspection. The animal was a sub-adult male. The cornea of the fellow eye was damaged and not suitable for investigation. The delay between the death of the animal

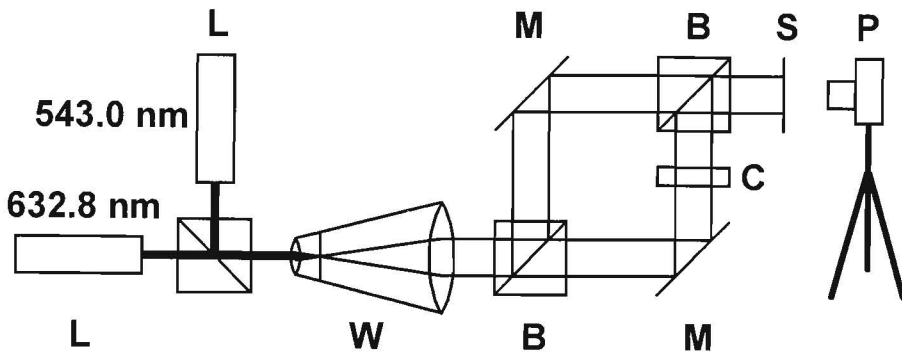


Figure 2. The two-wavelengths laser-interferometer. Wavefronts from two Helium-Neon-lasers, emitting light of 632.8 nm and 543.0 nm are combined to a single beam. The beam is then purified, widened, and split into two equal parts. One part of the beam passes through the measurement chamber while the other half serves as a reference beam and remains unchanged. Measurement and reference beams are combined again and create an interference pattern on the semi-transparent screen. The interference pattern can be photographed from behind the screen. B=beam splitters, C= measurement chamber, L=lasers, M=mirrors, P=camera, S=screen, W=beam purifier and widener.

and freezing of the eye is not known. Comparison with results from preliminary experiments gave no indication that the cornea studied in detail was aberrant in any respect.

Data analysis

Colour slides of the interference patterns were projected on a screen for evaluation. By placing red and green filters into the projection path we could again separate the colours of the two lasers.

If the phase difference (d) between the reference and the measurement wavefronts is known, refractive index (N) of the sample can easily be calculated as

$$N = N_{im} + d \cdot \lambda / D \quad (1)$$

with N_{im} =refractive index of the immersion medium (Tissue-Tek), λ =wavelength of the laser light (μm), D =thickness of the sample (μm).

Since the cornea samples had a higher refractive index than the immersion medium, light that passed through the sample is reaching the screen slightly later than light that missed the sample. This delay induced a phase difference in the wavefronts of light reaching the screen. The fraction (F) of the phase difference could easily be determined with an accuracy of about 1/10 of a wavelength by using the interference stripes in the surrounding immersion medium as guidelines. However, since we could not follow the interference stripes from the immersion medium into the cornea slices, it was unknown how many multiples (K) of the wavelength had to be added to obtain

$$d = F + K \quad (2)$$

It was furthermore unknown whether K was the

same for both wavelengths of light. Chromatic dispersion of ocular media increases with decreasing wavelength of light. Especially in thicker samples it had therefore to be expected that d might contain one or more additional multiples (dK) at 543 nm in comparison to results from measurements at 632.8 nm such that

$$d(543) = F(543) + K(632.8) + dK. \quad (3)$$

To determine K and dK we first assumed both to be 0. Refractive indices were converted such that $N'(543)$ was calculated from $N(632.8)$ and $N'(632.8)$ was calculated from $N(543)$. The conversion method is based on the known dispersive properties of ocular media in other vertebrate species (Kröger, 1992, equation (13)). Differences in refractive indices were determined as

$$dN(543.0) = \text{abs}(N(543.0) - N'(543.0)) \quad (4)$$

and

$$dN(632.8) = \text{abs}(N(632.8) - N'(632.8)). \quad (5)$$

Now K ($dK = \text{const.}$) could be found by minimizing dN in equations (4) and (5).

In slices of 14.8 μm thickness, relative phase difference between the two wavelengths ($d(543) - d(632.8)$) had to be less than one wavelength, i.e., $dK = 0$ with $F(543) > F(632.8)$. If one assumes $dK = 1$ ($D = 14.8 \mu\text{m}$), minimizing dN would result in a refractive index of about 1.75, which is much higher than the index of pure protein (ca. 1.56, Barer & Joseph, 1954), it is higher even than the refractive indices of most glasses. It is unreasonable to assume that such a high refractive index is possible in the harbor porpoise cornea.

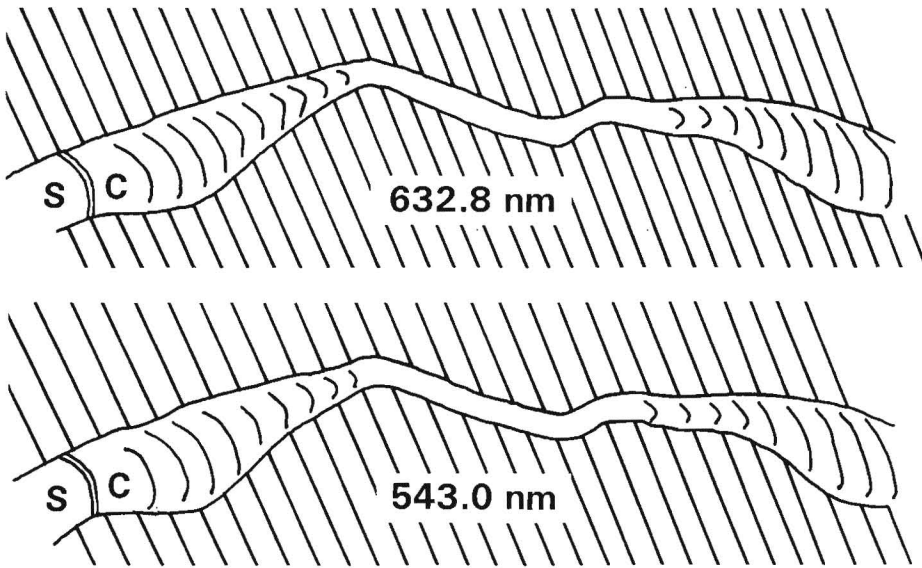


Figure 3. Interference patterns formed by two lasers of different wavelengths in a naso-temporal cross section of a harbor porpoise cornea drawn from a colour slide. Sample thickness was $14.8\ \mu\text{m}$. Only the centres of the thickened parts of the cornea (compare Fig. 1) were evaluated in detail. S=sclera, C=cornea.

Knowing the approximate value of the refractive index from the $14.8\ \mu\text{m}$ samples, we could also evaluate data obtained from slices thicker than $14.8\ \mu\text{m}$ by choosing $dK(D)$ such that $N(14.8) - N(D)$ were minimized.

The schematic eyes (Matthiessen, 1886; Kröger, 1989) and the ray-tracing model of the harbor porpoise eye (Kröger, 1989) were modified to incorporate the high refractive index found in the cornea. Since Kröger's measurements of the optical properties of the lens were done at $480\ \text{nm}$, refractive indices measured at $590\ \text{nm}$ were converted to $480\ \text{nm}$ with a method described by Kröger (1992, equation 13). The curvatures of the surfaces of the cornea, lens, and retina were determined from freeze cut sections and approximated by elliptical curves for the ray-tracing model. The cornea was slightly simplified by estimating a uniform, total index for the entire cornea. The estimates of the total refractive index of the cornea take into account that the surface index of the cornea is lower than the maximum index found in the interior of the cornea. However, the optics of diverging gradient index lenses are poorly understood so that a wide range of total refractive indices of the cornea was used in the model calculations.

Results

The method of two-wavelengths laser-interferometry was tested with two pieces of plastic

wrap of known thicknesses. Refractive indices were measured both with an Abbe refractometer ($n(632.8\ \text{nm}) = 1.4895 \pm 0.0006$, $N=8$; $n(543\ \text{nm}) = 1.4952 \pm 0.0003$, $N=8$) and with the laser-interferometer ($n(632.8\ \text{nm}) = 1.4885 \pm 0.0037$, $N=4$; $n(543\ \text{nm}) = 1.4946 \pm 0.0038$, $N=4$). The mean indices from both methods differed by less than 0.001 , the maximum difference was less than 0.003 for both wavelengths.

We evaluated interference patterns in the thicker part of the cornea where the spatial resolution of the method was sufficient. As far as the interference patterns could be followed towards the optical axis, there was no noticeable drop in refractive index of the most central strata of the cornea (Fig. 3). The region of the cornea closest to the optical axis could not be measured with the laser-interferometer. No further attempt was made to measure refractive index in the axial region of the cornea since, as outlined in the introduction, those areas are of little relevance to the optics of the harbor porpoise eye. Interference stripes were banded in the thickened part of the cornea, indicating a gradual increase of refractive index from the surfaces of the cornea to its interior (Fig. 3).

The refractive indices in Table 1 and Fig. 4 were calculated as the averages of N and N' . If one plots $dN(632.8, K)$ and $dN(543, K+dK)$ as functions of K , the minima in the curves for different wavelengths and sample thicknesses point to the measured refractive indices (Fig. 4). These indices

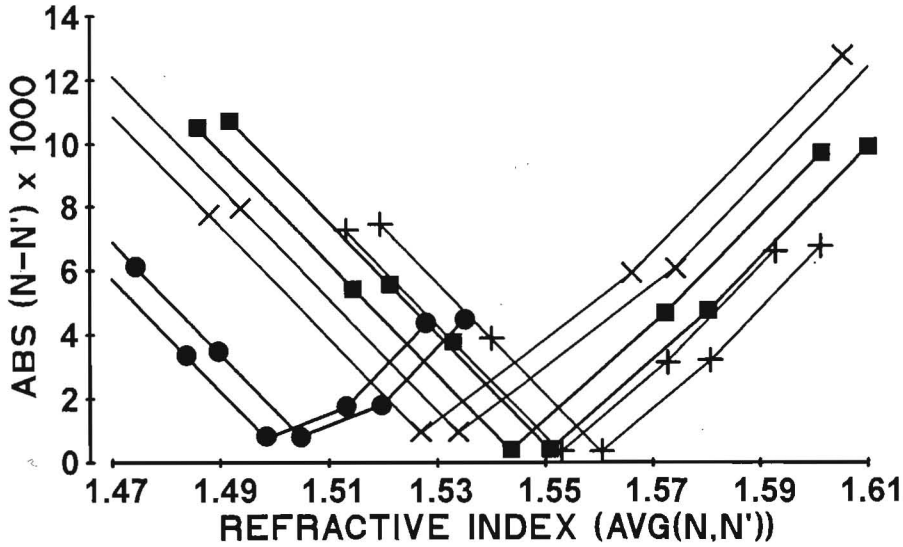


Figure 4. Evaluation of two-wavelength laser-interferometry. $\text{Abs}(N-N')$ is plotted against $\text{avg}(N, N')$ for different values of K . The minima point to the refractive indices of the samples. Curves corresponding to 543 nm are shifted to the right in comparison to the data for 632.8 nm due to the higher refractive index at the shorter wavelength. Sample thicknesses (μm): $x=14.80$, squares= 20.13 , $+ = 29.27$, circles= 39.20 .

are listed in Table 1. Refractive index is usually measured at 590 nm (e.g. Longhurst, 1973). Converting our average maximum refractive index to that wavelength results in a maximum refractive index of the cornea of 1.5330.

If a cornea with high refractive index is incorporated into the schematic eyes for the harbor porpoise by Matthiessen (1886) and Kröger (1989), both models predict a very slight hypermetropia (farsightedness) for paraxial optics (Table 2). Ray-tracing model calculations with an aspherical curvature of the posterior surface of the cornea (Kröger & Kirschfeld, 1992, Table 2) show that the harbor porpoise eye is close to emmetropia for most of the visual field (Fig. 5) if the total refractive index of the cornea is in the range from 1.50 to 1.53 at 480 nm ($\cong 1.49$ to 1.52 at 590 nm).

Discussion

Since the result of our experiments is a surprisingly high refractive index in the interior of the harbor porpoise cornea, it is advisable to discuss possible sources of experimental error that could have biased the results.

Error analysis

Measurements of the refractive indices of the surfaces of cetacean corneas with an Abbe refractometer range from 1.3653 to 1.3960 (Matthiessen, 1893, Kröger, 1989). The highest values were found

for the anterior surface in necrotic eyes where the outermost layers of the cornea had flaked off such that deeper layers of the cornea were exposed. Refractive indices of the intact interior surfaces of harbor porpoise corneas measured by Kröger (1989) averaged at 1.3673 (S.D.=0.0002, $N=4$). That is well within the range from 1.360 to 1.375 typically found in vertebrate corneas (e.g. Sivak & Mandelman, 1982). Therefore, freezing and thawing of the eyes apparently did not have a notable effect on the refractive index of the cornea.

The refractive index of biological samples is closely correlated with protein concentration (Barer & Joseph, 1954). Therefore, care was taken to keep the cornea sections moist throughout the entire procedure. We are confident that the large difference between surface index measurements with an Abbe refractometer and the index of the interior of the cornea measured with the laser-interferometer was not caused by dehydration of the samples. If one assumes that the cornea was swollen during our measurements, the real refractive index of the cornea would be even higher than suggested by our results.

We estimate that the method of converting refractive indices between wavelengths (Kröger, 1992) is accurate within ± 0.001 in the range between 543 and 632.8 nm. Inaccuracies of that magnitude cannot shift the minima in dN to other values of K since the second lowest values of dN in all but one case are at least 0.002 higher (Fig. 4).

Table 1. Maximum refractive indices in the harbor porpoise cornea at two wavelengths determined by laser interferometry

	Wavelength	
	632.8 nm	543.0 nm
Refractive index of the immersion medium:	1.3537	1.3568
Sample thickness:		14.80 μm
Number of data points:		5
Fraction of phase difference:	0.04 \pm 0.06	0.84 \pm 0.06
Multiples of wavelength:	4	4
Refractive index:	1.5269 \pm 0.0020	1.5339 \pm 0.0020
Sample thickness:		20.13 μm
Number of data points:		3
Fraction of phase difference:	0.03 \pm 0.19	0.20 \pm 0.24
Multiples of wavelength:	6	7
Refractive index:	1.5434 \pm 0.0041	1.5508 \pm 0.0042
Sample thickness:		29.27 μm
Number of data points:		5
Fraction of phase difference:	0.20 \pm 0.08	0.98 \pm 0.09
Multiples of wavelength:	9	10
Refractive index:	1.5528 \pm 0.0014	1.5603 \pm 0.0014
Sample thickness:		39.20 μm
Number of data points:		3
Fraction of phase difference:	-0.07 \pm 0.14	0.70 \pm 0.24
Multiples of wavelength:	9	10
Refractive index:	1.4983 \pm 0.0019	1.5046 \pm 0.0020
Average maximum refractive index of the cornea:	1.5303 \pm 0.0207	1.5374 \pm 0.0212

Since we could not measure the thickness of the cornea slices directly, we had to rely on our knowledge on the step size of the feed of the crystal. At least 2 test cuts were discarded before the subsequent slice was taken into investigation. Any error in slice thickness would result in a corresponding misreading in the refractive index of about the same, relative magnitude. Overestimating slice thickness would result in a lower than actual refractive index and vice versa. We estimate the possible error from this source to be less than 10%. Larger errors in slice thickness would have been detected by a visible difference in surface area between the face of the cornea in the sectioning block and the slice in the measurement chamber.

Opacity of the cornea slices increased rapidly with increasing thickness such that clearest interference patterns within the samples were obtained in slices of 14.8 μm thickness. We therefore regard the corresponding refractive index, which is close to the average of all data, as the most reliable value in our data (Table 1). The opacity of the slices most probably stemmed from disturbances of the collagen fiber matrix in the cornea that occurred during preparation of the slices. Cloudiness of the cornea was minor after dissection of the eye and before the cornea was freeze embedded.

Standard deviations for the refractive index of the cornea listed in Table 1 have to be interpreted carefully since they may give a misleading impression of the accuracy of the method. Especially in

thicker samples, slightly different data on the fractions of the phase differences can lead to considerably different interpretations by calling for more or fewer multiples (K) of the wavelength in the total phase difference (eqns. 2 and 3). Sources of error are thus not only measurement uncertainty in the fraction of phase difference, which is correctly quantified by the corresponding standard deviations, but also uncertainty in the number of wavelengths (K) added to the fraction of phase difference. This uncertainty is particularly noteworthy if the minimum in dN is not clearly defined, as in our 39.2 μm samples. Furthermore, measurements of refractive index at the two wavelengths are dependant of each other so that an error in the fraction of the phase difference at one wavelength will influence the results at both wavelengths (see eqns. 4 and 5). However, even if we assume the most extreme cases our data allow for, maximum refractive index of the harbor porpoise cornea would be in the range of 1.48 to 1.58, i.e., the lower limit would still be considerably higher than the surface index.

The cornea as a lens

It is a conservative proposition that the maximum refractive index in the thickened peripheral regions of the harbor porpoise cornea is in the range of 1.50 or even somewhat higher. An index of that magnitude provides the harbor porpoise cornea with the potential of considerable refractive power even in

Table 2. Eye models for the harbor porpoise

Schematic eyes: Source:	Matthiessen (1886) ($\lambda=590$ nm)	Kröger (1989) ($\lambda=480$ nm)
Refractive indices:		
sea water:	1.3393	1.3440*
cornea:	1.3670** (1.52)	1.3729 (1.53)
aqueous/vitreous:	1.3361	1.3420
lens (total index):	1.6323	1.6381
Cornea:		
anterior radius:	17.0	14.3
posterior radius:	10.7**	8.8
centre of curvature:	11.5**	9.6
Lens:		
anterior radius:	5.25	4.97
centre of curvature:	6.25	6.07
posterior radius:	5.25	4.69
centre of curvature:	4.75	4.59
Retina: position of vertex:	20.5	19.3
Focal point position:	19.85 (20.66)	18.54 (19.44)

The ray-tracing model. All surfaces are represented by elliptical curves:

Cornea:			
anterior axial radius:	13.50	anterior naso-temporal radius:	13.50
posterior axial radius:	3.93	posterior naso-temporal radius:	6.14
thickness at vertex:	0.60	refractive index (480 nm):	1.50 to 1.53
Lens:			
anterior axial radius:	3.92	posterior axial radius:	- 4.26
naso-temporal radius:	4.51	position of centre:	5.02
Retina:			
nasal radius:	12.5	temporal radius:	13.6
axial radius:	- 11.2	position of centre:	8.1
Pupil radius (dilated):	3.95		

Schematic eyes for the harbor porpoise based on measurements by Matthiessen (1886) and Kröger (1989) and the ray-tracing eye model modified after Kröger (1989). All positions are measured in mm from the anterior vertex of the cornea (ordinate) and from the optical axis (abscissa).

Schematic eyes: Focal point positions in parentheses are results obtained with the total refractive index of the cornea set to 1.52 (590 nm) and 1.53 (480 nm).

Ray-tracing: The model uses the same refractive indices for sea water and the aqueous and vitreous humors as the schematic eye by Kröger. The refractive index distribution within the crystalline lens was given by $n(r) = ((2 - r/R)^a)^{1/b} / b + c$, where R is the lens radius and a, b, and c are real numbers that were determined by fitting the function to the data on refractive index within the lens by Matthiessen (1886). Zones of equal refractive index in the lens were concentric ellipsoids so that R was different for the axial and equatorial dimensions. Corneal shape was analysed in detail in a different animal and scaled to the size of the original ray-tracing model.

*Kröger did not measure the refractive index of sea water, but used Matthiessen's value and converted it to 480 nm.

**Matthiessen did not measure the refractive index, the posterior radius, and the thickness of the cornea. We used values from Kröger's schematic eye and adjusted them to the size of the eye studied by Matthiessen. Matthiessen entirely neglected the cornea in his calculation and found even more myopia (focal point at 19.60 mm).

water. The effect may be enhanced by the gradient of refractive indices within the cornea. Due to the stronger curvature of the posterior surface (Fig. 1) the cornea acts as a diverging lens.

The slight hypermetropia predicted by the schematic eyes (Table 2) may be due to an overestimation of the curvature of the posterior surface of the cornea in the axial region. Since the curvature of the posterior corneal surface is notably aspherical (Fig.

1), the total refractive power of the cornea cannot be calculated easily. It is lower for paraxial rays and it changes depending on the direction of incident light, being higher for oblique directions. The effects of the aspherical curvature of the posterior surface of the cornea have been investigated in comparison to spherical models in more detail elsewhere (Kröger & Kirschfeld, 1992). Fig. 5 shows that the present model predicts an emmetropic

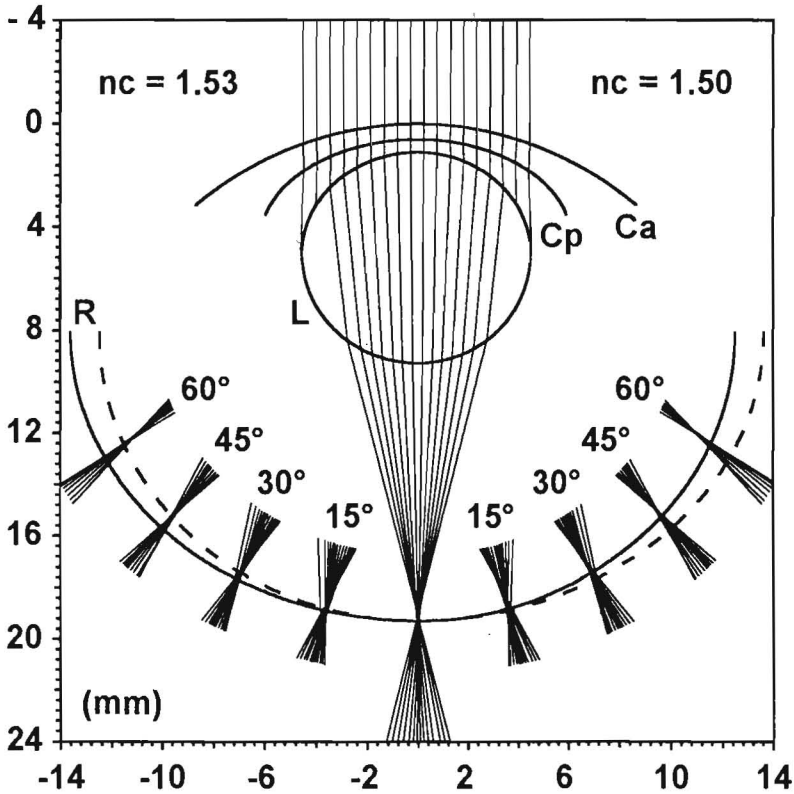


Figure 5. Results from ray-tracing model calculations. Bundles of parallel rays of varying inclination to the optical axis were traced through the eye model in Table 2 with $\lambda = 480$ nm. Except for the axial bundle, only the focal areas are shown. The dashed line is a mirror image of the asymmetrical retinal plane. The harbor porpoise eye is of egg-like shape with elongation of the bulbus towards the temporal (caudal) pole. Ray paths on the left hand side of the graph were calculated with the refractive index of the cornea set to 1.53 (480 nm). The axial bundle and the rays on the right hand side were traced with the refractive index of the cornea set to 1.50. Note that the focal points are close to the retinal plane for most angles of incident light. Increasing the total refractive index of the cornea from 1.50 to 1.53 has little effect on the refractive state of the eye. On the temporal side, the foci are proximal to the retinal plane, indicating myopia for nasal (rostral) directions of view. Ca (Cp)=anterior (posterior) surface of the cornea, L=crystalline lens, R=retina. The coordinate system originates in the anterior vertex of the cornea.

refractive state of the eye over most of the visual field. Increasing myopia for nasal (rostral) directions of view is due to elongation of the bulbus on the temporal (caudal) side (Fig. 5).

Conclusion

The cetacean cornea has to withstand an intraocular pressure that may be three to four times higher than in humans (Dawson, 1980). Although intraocular pressure has only been measured in the bottlenose dolphin (*Tursiops truncatus*), strong similarities in the anatomy of the eyes suggest that high intraocular pressure may be a common feature

of most cetacean eyes. Additional physical strain stems from fast swimming and breaching. It is therefore not surprising that the cetacean cornea consists of extremely tough tissue. The refractive index of 1.533 would translate into a protein concentration of about 81 percent by volume (Barer & Joseph, 1954) in the densest part of the cornea. High protein contents may serve a dual purpose in bringing about the high refractive index and the physical strength of the cornea.

Our results offer a plausible solution for the conflict between the apparent myopia of the harbor porpoise eye, based on past investigations of the refractive state, and the obvious usefulness of vision

to the animals. Except for some aberrant freshwater dolphins, extended thickening in the periphery of the cornea has been found in all cetacean species studied so far (e.g. Matthiessen, 1893, *Megaptera novaeangliae*, *Balaenoptera musculus*, Pütter, 1903, *Balaenoptera physalus*, *Balaena mysticetus*, *Phocoena phocoena*, *Delphinapterus leucas*, *Hyperoodon* sp., Rochon-Duvigneaud, 1940, *Delphinus delphis*, *Phocoena phocoena*, *Physeter macrocephalus*, *Megaptera novaeangliae*, Mann, 1946, *Balaenoptera physalus*, *Physeter macrocephalus*). It may therefore be a general pattern that the corneas of whales act as diverging lenses in underwater viewing conditions. Additional, positive refractive power has to reside in the crystalline lens to achieve an emmetropic refractive state of the eye. It is an interesting question what the evolutionary advantage of this apparent paradox might be.

Acknowledgements

We wish to thank Chris Smeenk, Rijksmuseum van Natuurlijke Historie, Leiden, and Carl Chr. Kinze, Naturhistorisk Museum, Copenhagen, for collecting the eyes used in this study. This work was supported by a post-doctoral scholarship from the Max-Planck-Gesellschaft to R. H. H. Kröger.

References

- Barer, R. & Joseph, S. (1954) Refractometry of living cells. Part I. Basic principles. *Quart. J. Micr. Sci.* **95**, 399–423.
- Dawson, W. W. (1980) The cetacean eye. In *Cetacean behavior: Mechanisms and functions* (ed. Herman L. M.). Wiley, New York, pp. 51–100.
- Dawson, W. W., Schroeder, J. P. & Dawson, J. F. (1987a) The ocular fundus of two cetaceans. *Marine Mammal Sci.* **3**, 1–12.
- Dawson, W. W., Schroeder, J. P. & Sharpe, S. N. (1987b) Corneal surface properties of two marine mammal species. *Marine Mammal Sci.* **3**, 186–197.
- Dral, A. D. G. (1972) Aquatic and aerial vision in the bottlenosed dolphin. *Neth. J. Sea Res.* **5**, 510–513.
- Dral, A. D. G. (1975) Some quantitative aspects of the retina of *Tursiops truncatus*. *Aquatic Mammals* **2**, 28–31.
- Dral, A. D. G. (1977) On the retinal anatomy of Cetacea (mainly *Tursiops truncatus*). In *Functional anatomy of marine mammals*, Vol. 3. (ed. Harrison R. J.). Academic, London, pp. 81–134.
- Dral, A. D. G. (1983) The retinal ganglion cells of *Delphinus delphis* and their distribution. *Aquatic Mammals* **10**, 57–68.
- Duke-Elder, S. (1958) System of ophthalmology, Vol. 1: The eye in evolution. Klimpton, London.
- Kröger, R. H. H. (1989) Dioptrik, Funktion der Pupille und Akkommodation bei Zahnwalen. Ph. D. Dissertation, Universität Tübingen.
- Kröger, R. H. H. (1992) Methods to estimate dispersion in vertebrate ocular media. *J. Opt. Soc. Am. A* **9**, 1486–1490.
- Kröger, R. H. H. & Kirschfeld, K. (1992) The cornea as an optical element in the cetacean eye. In *Marine mammal sensory systems*. (eds Thomas, J. A., Kastelein, R. A. & Supin, A. Ya.). Plenum, New York, pp. 97–106.
- Longhurst, R. S. (1973) Geometrical and physical optics (3. edition). Longman, London.
- Mann, G. F. (1946) Ojo y vision de las ballenas. *Biologica* **4**, 23–71.
- Mass, A. M., Supin, A. Ya., & Severtsov, A. N. (1986) Topographic distribution of sizes and density of ganglion cells in the retina of a porpoise, *Phocoena phocoena*. *Aquatic Mammals* **12**, 95–102.
- Mass, A. & Supin, A. (1990) Best vision zones in the retinae of some cetaceans. In *Sensory abilities of cetaceans*. (eds Thomas, J. A. & Kastelein, R. A.). NATO ASI Series A: Life Sciences Vol 196. Plenum, New York, pp. 505–517.
- Matthiessen, L. (1886) Ueber den physikalisch-optischen Bau des Auges der Cetaceen und der Fische. *Pflüger's Arch.* **38**, 521–528.
- Matthiessen, L. (1893) Ueber den physikalisch-optischen Bau der Augen vom Knölwal (*Megaptera boops*, Fabr.) und Finwal (*Balaenoptera musculus*, Comp.). *Z. vergl. Augenheilk.* **7**, 77–101.
- Pütter, A. (1903) Die Augen der Wassersäugethiere. *Zool. Jb., Anat.* **17**, 99–402.
- Rochon-Duvigneaud, A. (1940) L'oeil des cetaces. *Arch. Mus. Nat. Hist., Ser. 6*, **16**: 57–90.
- Sivak, J. G. & Mandelman, T. (1982) Chromatic dispersion of the ocular media. *Vision Res.* **22**, 997–1003.
- Walls, G. (1942) The vertebrate eye and its adaptive radiation. McGraw-Hill, New York.